Niobium phosphates as an intermediate temperature proton conducting electrolyte for fuel cells

Huang, Yunjie; Li, Qingfeng; Jensen, Annemette Hindhede; Yin, Min; Jensen, Jens Oluf; Christensen, Erik; Pan, Chao; Bjerrum, Niels; Xing, Wei

Published in:
Journal of Materials Chemistry

Link to article, DOI:
10.1039/c2jm34704k

Publication date:
2012

Document Version
Publisher's PDF, also known as Version of record

Journal of Materials Chemistry

Dynamic Article Links

Cite this: J. Mater. Chem., 2012, 22, 22452

www.rsc.org/materials

PAPER

Niobium phosphates as an intermediate temperature proton conducting electrolyte for fuel cells

Yunjie Huang,[a] Qingfeng Li,*[a] Annemette H. Jensen,[a] Min Yin,[ab] Jens Oluf Jensen,[a] Erik Christensen,[a] Chao Pan,[a] Niels J. Bjerrum[a] and Wei Xing*[b]

Received 9th February 2012, Accepted 29th August 2012
DOI: 10.1039/c2jm34704k

A new proton conductor based on niobium phosphates was synthesized using niobium pentoxide and phosphoric acid as precursors. The existence of hydroxyl groups in the phosphates was confirmed and found to be preserved after heat treatment at 500 °C or higher, contributing to an anhydrous proton conductivity of 1.6×10^{-2} S cm^{-1} at 250 °C. The conductivity increased with water content in the atmosphere and reached 5.8×10^{-2} S cm^{-1} under pure water vapour at the same temperature. The conductivity showed good stability in the low water partial pressure range of up to 0.05 atm. The metal phosphates are of high interest as potential proton conducting electrolytes for fuel cells operational in an intermediate temperature range.

1. Introduction

Great efforts are being made to develop new proton conducting materials as electrolytes for fuel cells operational at intermediate temperatures from 200 to 400 °C.[1–14] This temperature range is of strategic importance, since it bridges the gap between the currently available high and low temperature fuel cells. A number of biofuels can be directly oxidized or reformed to hydrogen *via* an internal reformer in this temperature range. Electrode kinetics will be significantly enhanced so that it may be possible to use non-noble metal catalysts. On the other hand, this temperature range is low enough to permit the use of a wide selection of construction materials which may allow for simplified cell and stack construction as well as low costs and long-term durability.

Proton conductors with conductivities of above 10^{-2} S cm^{-1}, especially under low water content in the atmosphere, are key materials to achieve intermediate temperature operation of fuel cells.[1,2] It has long been known that several oxyacid salts, typically phosphates, exhibit promising proton conductivities in this temperature range. Of special interest are pyrophosphates *e.g.* SnP_2O_7, which, often doped with other metals such as In^{3+}, exhibit high conductivities (>10^{-2} S cm^{-1}) at temperatures of up to 300 °C under unhumidified conditions.[10–13] Research has also been done to develop proton conducting materials including ammonium polyphosphates, caesium hydrogen phosphates as well as other phosphate composites, as recently reviewed by Paschos *et al.*.[14]

Hydrated niobium oxides (niobic acids) are known to possess strong surface acidity because of the existence of both Lewis and Brønsted acid sites.[15] They are therefore used as solid acid catalysts for acid-catalyzed reactions such as esterification, polycondensation and dehydration reactions.[15–19] The relatively small number of acid sites as well as unstable surface acidity at elevated temperatures were however found to restrict the catalytic applications. As reported by Nowak and Ziolek,[15] the surface acidity greatly decreased at temperatures higher than 700 K[15] and almost disappeared at 873 K.[20]

Niobium phosphates have on the other hand shown higher surface acidities than the niobic acids.[16] Most importantly, the surface acidity of niobium phosphates can be preserved in the above mentioned temperature range.[21–23] Niobium oxide phosphate ($NbOPO_4$), for example, is known to have a layered structure, in which a distorted NbO_6 octahedron is connected to PO_4 tetrahedra *via* shared corners.[24] This structure allows for intercalation of guest molecules such as alcohols, amines, water and acids *e.g.* sulphuric and phosphoric acids, most likely involving hydrogen bonding in many of the cases.[16,24] Da Silva *et al.*[21] showed the distinct existence of both Lewis and Brønsted acid sites in a $NbOPO_4$ surface that had been heat treated at 400 °C. Another interesting report by Florentino *et al.*[23] compared the acidic and catalytic properties of niobium oxide with those of niobium phosphate in which the molar ratio of P to Nb was about 1.5 : 1. It was shown that the strong acid sites were preserved more stably on the phosphate than on the oxide during the heat treatment. As a result, niobium phosphates exhibited remarkable activity in acid-catalyzed reactions and could be used in a higher temperature range. Alternatively, the phosphoric acid treatment of niobic acid has also been proposed as an effective

[a]*Department of Energy Conversion and Storage, Technical University of Denmark, Kemitorvet 207, DK-2800, Lyngby, Denmark. E-mail: qfli@dtu.dk; Fax: +45 4588 3136; Tel: +45 4525 2318*
[b]*Laboratory of Advanced Power Sources, Changchun Institute of Applied Chemistry, Chinese Academy of Sciences, Changchun, 130022, P. R. China. E-mail: xingwei@ciac.jl.cn; Fax: +86 431 8526 2223; Tel: +86 431 85262225*

approach to enhance the stability of the surface functionalities at high temperatures.[15,25,26] As shown by Okazaki *et al.*[25] the surface acidity and catalytic activity of the phosphoric acid treated niobic acid catalysts were well maintained at temperatures as high as nearly 873 K, attributable to the presence of non-volatile polyphosphates formed by the condensation of phosphoric acid on and near the surface of the niobic acid.

In view of the easy adsorption of water and preserved hydrogen bond networks in the niobium phosphates, even at relatively high temperatures, niobium phosphate would be a good candidate material for proton conduction. Cantero *et al.*[27] was the first to prepare acidic niobium phosphates, in the form of $NbOPO_4 \cdot nH_2O$ ($n < 3$), and measure their proton conductivities over a relatively low temperature range from 27 to 140 °C (most likely under atmospheric humidity but the humidity was not specified by the authors). The conductivity was found to increase with temperature below 100 °C but decrease at higher temperatures. The highest conductivity of 5×10^{-6} S cm^{-1} was achieved at around 100 °C and attributed to the presence of water species in the interlayer space of the phosphates. Recently, Chai *et al.*[28] synthesized niobium phosphates using niobium chloride and phosphoric acid as precursors. The phosphates obtained had amorphous structures with uniform and nano-sized particles. They determined a proton conductivity of about 1.7×10^{-2} S cm^{-1} at room temperature under a relative humidity of 100% and a pressure of 360 MPa. Fuel cell tests in H_2/O_2 mode at room temperature and direct methanol mode at 60 °C were also conducted.

In the present work, niobium phosphates were synthesized from phosphoric acid and niobium pentoxide. To the best of our knowledge, it is the first report that the resulting niobium phosphates possess a proton conductivity of the 10^{-2} S cm^{-1} level under a dry atmosphere and higher conductivities under humidified conditions in an intermediate temperature range with reasonably good stability.

2. Experimental

2.1 Chemicals and preparation

Nb_2O_5 and H_3PO_4 (85 wt%) were used as received from Aldrich Co. Silver paste (type LOCTITE® 3863) was supplied by Henkel Co. Deionized water was used for humidification during the conductivity measurements.

Nb_2O_5 was first mixed with H_3PO_4 at 200–300 °C under mechanical stirring until a viscous paste was obtained. The initial molar ratio of P/Nb was 2.5 : 1. The paste was divided into four portions and heat treated in alumina crucibles at 350 °C, 500 °C, 650 °C and 800 °C for 3 h. The obtained solids were then ground with a mortar and pestle. The prepared niobium phosphates are hereafter referred to as NbP350, NbP500, NbP650 and NbP800, respectively.

2.2 Material characterizations

The crystalline structures of the prepared niobium phosphates were characterized using X-ray diffraction (XRD) using a Huber G670 X-ray diffractometer with a copper rotating anode (CuK radiation, $\lambda = 1.54056$ Å). FT-IR spectra of the phosphate powders were recorded on a PerkinElmer 1710 spectrometer under ambient atmosphere. Thermogravimetric (TG) and differential thermal analysis (DTA) were performed using a Netzsch STA 409 PC system. Air was used as the purge gas and the samples were heated at a rate of 10 °C min^{-1}. Scanning electron microscopy (SEM) measurements were performed on a Carl Zeiss EVO MA10 microscope.

2.3 Conductivity measurements

For conductivity measurements, the phosphate powders were first pressed into pellets with a diameter of 13 mm and a thickness of about 2 mm under a pressure of 5×10^3 kg cm^{-2}. Each side of the pellet was uniformly coated with a thin layer of silver paste. A gold mesh with the same area as the pellet was placed on each side of the pellet. The assembly was held together by two porous SiC disks in order to allow for access of the humidified air and contained in a stainless steel chamber (the conductivity cell) with an inlet and outlet for air flow of controlled humidity. Two silver wires were connected to the gold meshes for the electrical measurements. The humidity of the air flow was controlled by means of a water pump (Prominence LC-20AD, Shimadzu Co.) and air flow meter through an evaporator. Both the conductivity cell and the evaporator were placed in the same furnace for temperature control. Electrochemical impedance spectroscopy (Princeton VERSASTAT 3) was used for the conductivity measurements with frequency in a range of 1–10^6 Hz and an ac amplitude of 10 mV. The conductivity was determined by the intercept on the real axis at the high frequency region in the complex plane. During the measurements, the temperature of the furnace was increased for the first heating cycle from room temperature to 250 °C with a heating rate of 2 °C min^{-1}, followed by a cooling cycle after the sample had been kept at 250 °C for 30 min. The conductivity was recorded as a function of temperature during both heating up and cooling down cycles. The conductivity was subsequently measured at a constant temperature of 250 °C with varied water content in the atmosphere. Finally, the conductivity stability was evaluated at 250 °C under dry air (*i.e.* unhumidified air decompressed from 7 bar, subsequently referred to as "dry air") or humidified air with a water partial pressure of 0.05 atm.

2.4 Electromotive force (EMF) and open circuit voltage (OCV) measurements

A cell was assembled with gas diffusion electrodes on each side of a phosphate pellet as electrolyte for measurements of the EMF and OCV. The electrodes were prepared by spraying a catalyst ink onto carbon cloth. The ink consisted of carbon supported platinum catalysts and polybenzimidazole in formic acid. To improve the mechanical strength of the pellet, 20 wt% of polybenzimidazole was added as a binder during the pressing. For EMF measurements the cell was fed with pure hydrogen on one side and a mixture of hydrogen and nitrogen (with a partial pressure of hydrogen of 0.05 atm) on the other side. The EMF was measured as a function of temperature from 70 °C to 230 °C and compared with the theoretical values calculated using the Nernst equation. The proton transference number was calculated as the ratio between the measured and calculated values. For

OCV measurements the cell was operated with hydrogen and air on each side at 70, 110 and 200 °C, respectively.

3. Results and discussion

3.1 X-Ray analysis

Fig. 1 shows the X-ray diffraction patterns of the phosphates heat treated at different temperatures. For comparison, the histogram patterns of three different crystal structures of niobium phosphates *i.e.* orthorhombic $Nb_{1.91}P_{2.82}O_{12}$ (JCPDS 83-415), cubic $Nb_2P_4O_{15}$ (JCPDS 28-715) and monoclinic $Nb_5P_7O_{30}$ phases (JCPDS 48-840) are also given in the same figure. The patterns of NbP350 and NbP500 can be indexed as a mixture of orthorhombic $Nb_{1.91}P_{2.82}O_{12}$ and monoclinic $Nb_5P_7O_{30}$ phases while the other two samples (NbP650 and NbP800) have a mixture of monoclinic $Nb_5P_7O_{30}$ and cubic $Nb_2P_4O_{15}$ phases. By comparing the relative intensity of the diffraction peaks, one could conclude that higher heat treatment temperatures induced more formation of the cubic $Nb_2P_4O_{15}$ phase. Comparison of the molar ratio of P/Nb (2.5 : 1) in the initial precursor and the obtained crystalline phosphates indicated the possible existence of amorphous phosphorus-containing phases in the phosphates. It had been considered that the conductivity of SnP_2O_7-based proton conductors depended on the synthetic history. The resultant phosphates from the metal oxide and phosphoric acid[12,13] exhibited a high conductivity of above 0.1 S cm^{-1} while those prepared by an aqueous solution method[29] showed a conductivity of several orders of magnitude lower. It was suggested that the excess phosphoric acid in the preparation promoted the formation of a secondary amorphous phase in grain boundaries, which was considered to provide additional pathways for proton transport,[30] and therefore significantly enhance the conductivity.[14,29] The deficiency of the metal in the bulk phosphates seemed to enhance formation of proton-containing groups in the phosphates, which were suggested to be the origin of the anhydrous proton conductivity.

3.2 FT-IR spectra

Fig. 2 shows the FT-IR spectra of the prepared niobium phosphates. For all of the samples the characteristic features are the vibration of Nb–O–Nb[28] at 626 cm^{-1}, the symmetrical stretching vibration and asymmetrical stretching vibration of P–O–P[31,32] at 720 and 925 cm^{-1}, and the deformation and vibration modes of P–O[28,31] at 545 and 1070 cm^{-1}. Another important band is located around 1260 cm^{-1} and can be assigned to the P–O–H deformation mode,[28] indicating directly the existence of proton-containing groups in the prepared niobium phosphates.

In addition, there are four other broad bands between 1500 and 3800 cm^{-1} which might be attributed to the vibration of the bonded O–H groups and/or the adsorbed H–O–H groups. These absorption peaks for OH groups are well recognized for SnP_2O_7-based materials,[11,33] although the formation mechanism is not fully understood. The adsorption bands at 1650 and 3410 cm^{-1} were considered as the vibration and deformation modes of O–H groups.[11] The band at 2900 cm^{-1} could be from the vibration of hydrogen bonded O–H groups where protons are considered to migrate more easily.[33] These proton-containing species of O–H groups are of the most interest for the proton conductors. Nagao *et al.*[11] tried to draw out a relationship between the amount of protons and the anhydrous conductivity of SnP_2O_7-based conductors by comparing the absorbance intensity of peaks between 1650 and 3410 cm^{-1}. The characteristic peaks for proton-containing groups from FT-IR results combined with the stable anhydrous conductivity results shown in the following sections could be seen to demonstrate the existence of intrinsic protons in the phosphates. It is suggested that the formation of proton containing groups is attributed to the stable surface acidity even after high temperature treatments of the niobium oxide by phosphoric acid, as discussed above. On the other hand, there might be another formation mechanism of proton-containing species. For SnP_2O_7-based conductors, the following reactions between water molecules, lattice oxides and electron

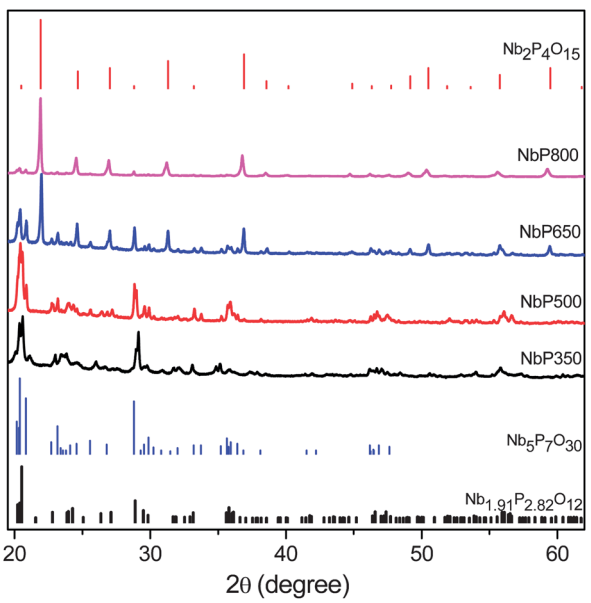

Fig. 1 XRD patterns of niobium phosphates sintered at different temperatures as indicated in the figure.

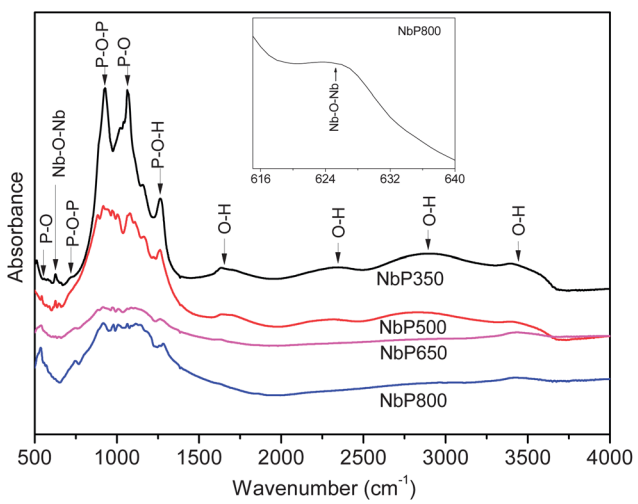

Fig. 2 FT-IR spectra of niobium phosphates heat treated at different temperatures as indicated in the figure.

holes or oxygen vacancies have been suggested,[11] which may also be of some importance for the present phosphate system:

$$H_2O + 2O_o^x + 2h^{\cdot} \leftrightarrow \tfrac{1}{2}O_2 + 2OH_o^{\cdot} \quad (1)$$

$$H_2O + 2O_o^x + V_o^{\cdot\cdot} \leftrightarrow 2OH_o^{\cdot} \quad (2)$$

Where O_o^x, $h^{\cdot}$, $V_o^{\cdot\cdot}$ and $OH_o^{\cdot}$ are the oxide ions at normal lattice sites, electron holes, oxygen vacancies and formed proton-containing group, respectively.

Another observation from FT-IR was that the relative absorbance intensity for the OH groups decreased with the heat treatment temperature, which, as discussed below, lowered the anhydrous conductivity.

3.3 TGA and DTA

The thermal stabilities of the prepared phosphates were studied by TGA and DTA, as shown in Fig. 3. For comparison, the TGA–DTA curve for phosphoric acid (85 wt%) is also presented in the figure. A small peak was seen in the DTA for phosphoric acid at temperatures of up to 150 °C, showing the loss of water at temperatures around the boiling point (156 °C) of the acid. Increasing the temperature further led to a steady decrease in the weight due to dehydration of the acid. A big plateau in the TGA at temperatures around 400–500 °C was observed, where the remaining weight corresponded to the formation of pyrophosphoric acid ($H_4P_2O_7$ at 77 wt%), tripolyphosphoric acid ($H_5P_3O_{10}$ at 74.6 wt%) or trimetalphosphoric acid ($H_3P_3O_9$ at 69.4 wt%). The steady weight loss in this temperature range was accompanied by an endothermic peak in the DTA. The content of phosphorus oxides (P_4O_{10}) in the acid was around 62 wt%, which was reached at about 600 °C with no visible plateau in the TGA, as the oxide gradually evaporated.

For NbP350, the phosphates that had been previously heat treated at 350 °C for 3 h, a slow decrease in the TGA curve starting from 150 °C was seen, showing the loss of water from the atmospheric adsorption and the remaining acid in the sample. At temperatures above 550 °C, a faster decrease in the weight occurred apparently in association with the loss of the phosphorus oxides, as compared with the TGA for phosphoric acid. During the preparation of niobium phosphates, excess phosphoric acid was used, which would lead to formation of amorphous oxides in the subsequent heat treatment. The metal phosphates by themselves are thermally stable in this temperature range. Cantero *et al.*[27] carried out TGA for $NbOPO_4 \cdot nH_2O$ ($n < 3$) which showed little weight loss at temperatures of up to 400 °C. The thermal stability of niobium phosphates was also observed for the phosphate samples with higher heat treatment temperatures. NbP500 showed a slight weight loss starting at above 300 °C while NbP650 and NbP800 had no visible weigh changes at temperatures of up to 550 °C, showing the elimination of unstable phosphorus-containing phases by the heat treatment. In all cases, a broad endothermic peak which decreased in height as the heat treatment temperature was elevated and peaked at about 530 °C was observed in DTA curves. This is assumed to be associated with the preserved hydroxyl groups in the prepared phosphate samples, which are essential for the anhydrous proton conductivity. It is clear that the heat treatment temperature should be optimized by considering the thermal stability and the preserved proton containing groups of the phosphates with a view to applications in the intermediate temperature range.

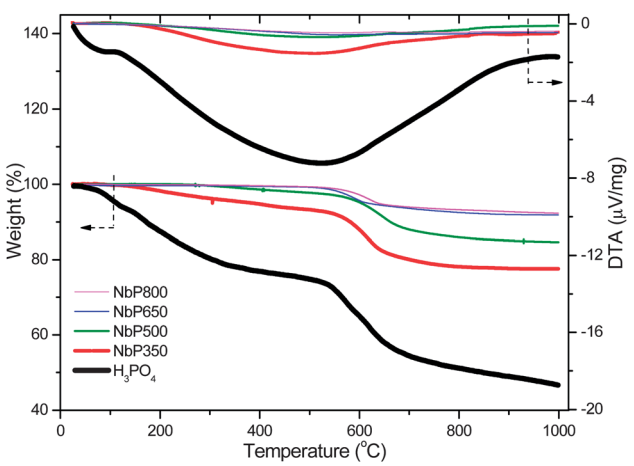

Fig. 3 TGA and DTA of the prepared niobium phosphates sintered at different temperatures and phosphoric acid.

3.4 SEM

The surface morphologies of the prepared niobium phosphates were characterized by SEM. As shown in Fig. 4, phosphates heat treated at relatively low temperatures (350 °C and 500 °C) were in particle clusters. Higher heat treatment temperatures resulted in particle aggregation of the phosphates. No distinct particles were visible on the surfaces of NbP650 and NbP800.

For metal pyrophosphates *e.g.* SnP_2O_7, it was reported that the high proton conductivity under anhydrous conditions depended on the synthetic history.[14,29] This is an indication that the possible existence of secondary amorphous phases in grain boundaries or pores may play a key role in proton conduction mechanisms. In other words, the surface morphology of both bulk phosphates and secondary phases would appreciably influence the conductivity. Chai *et al.*[28] reported that amorphous niobium phosphate with a particle size of about 20 nm showed proton conductivity of around 50 times higher than that of micro-sized amorphous niobium phosphate under 100% humidified conditions. In the present work, the micro-morphology of the phosphates may also be an issue affecting the conductivity, however, no efforts were made to explore the morphology optimization.

3.5 Conductivity

Fig. 5 shows the conductivity results of the prepared niobium phosphates under a dry air atmosphere. During the measurement, the temperature dependence of conductivity was first checked under heating–cooling cycles of the samples. For NbP350, the conductivity was found to be as high as 6.6×10^{-3} S cm^{-1} during the first heating cycle started from 70 °C. The conductivity increased to 2.4×10^{-2} S cm^{-1} at 160 °C. Further increasing the temperature, however, led to a steady decrease in the conductivity. After being held at 250 °C for 30 min, the remaining conductivity was only about 5.5×10^{-3} S cm^{-1}. In the

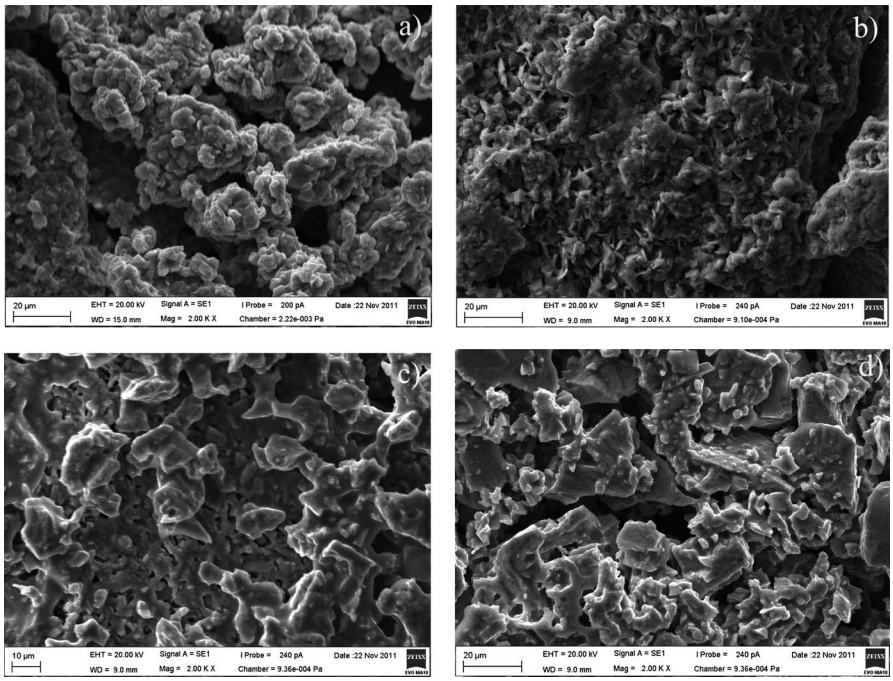

Fig. 4 SEM images of prepared niobium phosphate with different heat treatment temperatures: (a) 350 °C, (b) 500 °C, (c) 650 °C and (d) 800 °C.

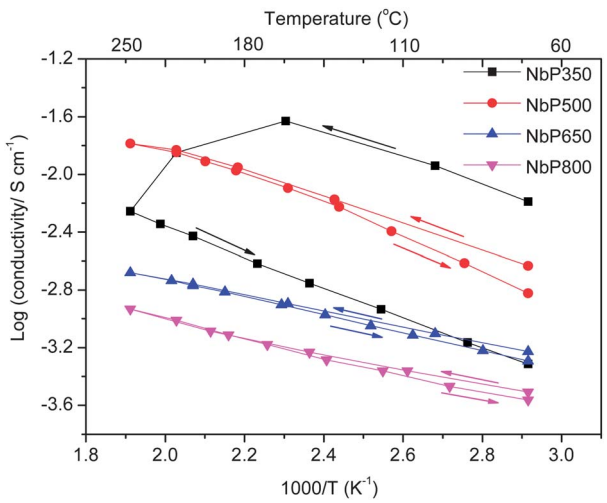

Fig. 5 Temperature dependence of conductivity for niobium phosphates under dry air. The arrows show the heating up and cooling down cycles of the measurements.

following cooling cycle, the conductivity was much lower than that of the first heating cycle. Apparently, the observed decrease in conductivity was due to elimination of the unstable OH groups in the high temperature range of the measurement, as evidenced in the above mentioned TGA results. These unstable OH groups also resulted in the high absorbance shown in the FT-IR spectra in Fig. 2.

By comparing the conductivity between heating and cooling cycles, it can be seen that the phosphates heat treated at 500 °C, 650 °C and 800 °C showed much better stability and reversibility than NbP350 treated at 350 °C. The conductivity of the heating cycle was only slightly higher than that of the cooling cycle in the temperatures below 150 °C, which could due to the remaining adsorbed water. It seems that the proton-containing groups existing in the phosphates treated at temperatures above 500 °C could be preserved and contribute to the anhydrous proton conductivity. In good agreement, Fig. 3 shows no visible weight losses in the corresponding TGA curves at temperatures around 250 °C for NbP500, NbP650 and NbP800. In other words, the heat treatment at high temperatures improved both thermal stability and conductivity preservation of the phosphates. However, it can also be seen from Fig. 5 that the conductivity decreased as the treatment temperature increased from 500 °C to 800 °C. Referring to the FT-IR spectra of Fig. 2, where less intensive absorbance for the proton-containing groups was observed for NbP500, NbP650 and NbP800, this steady decrease in conductivity was not a surprise. It is interesting to notice that a heat treatment temperature of above 500 °C gave a stable proton conductivity of as high as 1.6×10^{-2} S cm^{-1} at 250 °C under a dry atmosphere with a nearly recoverable performance during the thermal cycling.

Under a humidified atmosphere at 250 °C, the conductivity was found to significantly increase with the water partial pressure for all the prepared phosphates, as shown in Fig. 6. For NbP500, the conductivity increased from 1.6×10^{-2} S cm^{-1} to 2.8×10^{-2} S cm^{-1} when the atmosphere was changed from dry to humidified air with a water partial pressure of 0.05 atm. Under pure water vapour, a conductivity of as high as 5.8×10^{-2} S cm^{-1} was achieved. Through the water partial pressure range from 0 to 1, NbP500 showed the highest conductivity of the four samples. The conductivity improvement by the atmospheric humidification was obvious and could be attributed to the formation of external H-bonds[14] and/or proton containing species from the reaction between water, oxygen vacancies and the electron-holes,[11,34,35] as seen in reactions (1) and (2) above. As a result, in an atmosphere with a water vapour pressure as low as 0.05 atm,

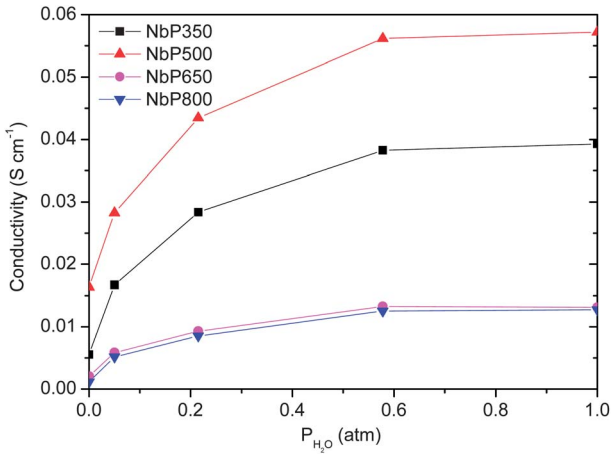

Fig. 6 Proton conductivity of niobium phosphates at 250 °C as a function of water partial pressure in the ambient pressure air.

which could be easily achieved with the water produced in the cathode air steam of an operating fuel cell, the niobium phosphate exhibited a conductivity of practical interest.

3.6 Conductivity stability

Further investigations were made to evaluate the conductivity stability of NbP500 and NbP650 at 250 °C under both dry and humidified air with a water partial pressure of 0.05 atm. As shown in Fig. 7, a steady decrease in the conductivity of NbP500 during the stability test was observed, with a greater decrease under dry air than under the slightly humidified atmosphere. After 50 h, 36% and 57% of the initial conductivity remained under the dry and humidified atmospheres, respectively. A much higher stability was observed for NbP650 compared with NbP500, though the initial conductivity was lower under both conditions. During a period of 50 h the remaining conductivity was found to be about 70% of the initial value. Most interestingly, the conductivity decrease during the stability test under both atmospheric conditions happened primarily within the first 10 h. For the rest of the period of measurement, the conductivity showed little change. These stable conductivities under dry air confirmed the preservation of the proton-containing groups in the phosphates even after the high temperature heat treatment during the preparation. The better conductivity preservation of NP650 concurred with the observed higher thermal stability of the phosphates as prepared by heat treatment at higher temperatures.

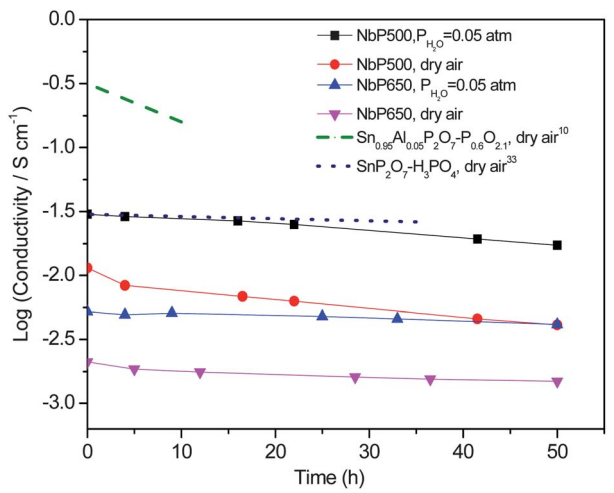

Fig. 7 Conductivity stability of NbP500 and NbP650 under dry air and humidified air with the water partial pressure of 0.05 atm at 250 °C. Dashed lines were taken from references as indicated in the figure.

The conductivity stability is in fact a concern for most of the phosphate-based proton conducting materials. However, limited information is available even for the most extensively studied SnP_2O_7-based systems. Heo *et al.*[10] reported a 50% decrease in conductivity for $Sn_{0.95}Al_{0.05}P_2O_7$–$P_{0.6}O_{2.1}$ after being kept in a dry atmosphere for 10 h, whereas Xu *et al.*[33] reported a higher stability for the SnP_2O_7–H_3PO_4 system. These results are also included in Fig. 7 for comparison. Further doping of the phosphates with metal ions of different valencies might further improve both the conductivity and the stability; a systematic investigation of this is underway.

3.7 EMF and OCV measurements

Efforts were made to assemble a cell by pressing the niobium phosphates into an electrolyte pellet, onto which platinum gas diffusion electrodes were attached. Under operation with hydrogen on both sides at different partial pressures, the EMF of a concentration cell was measured as shown below:

$$H_2\ (1\ atm),\ Pt\ |NbP500|\ Pt,\ H_2\ (0.05\ atm) \qquad (3)$$

The EMF obtained as a function of temperature is shown in Fig. 8. It can be seen from the figure that the obtained EMF was very close to the theoretical values calculated from the Nernst equation. The ratio of the measured EMF to the theoretical value was assumed to be the proton transference number[30,34] and was found to be between 0.97 and 0.98. This indicated the protonic nature of the ionic conductivity of the niobium phosphates. As shown in Fig. 9, OCV as high as 1.045 V was observed at 70 °C. At higher temperatures, 110 °C and 200 °C, OCVs were measured as 0.895 V and 0.863 V, respectively. The decrease in OCV at elevated temperatures was assumed to be associated mainly with sealing difficulties, Pt oxidation and decrease in the

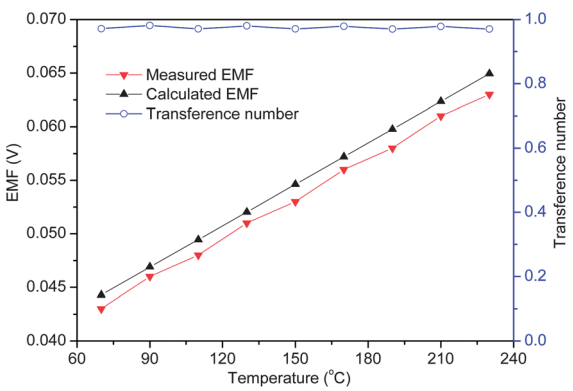

Fig. 8 EMF values and proton transference numbers for a hydrogen concentration cell with NbP500 as electrolyte.

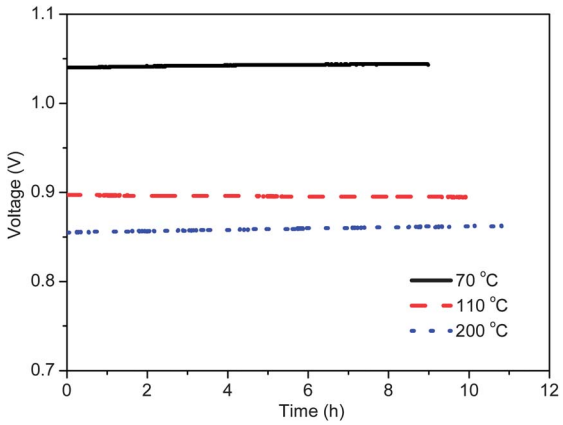

Fig. 9 OCV for a hydrogen/air cell with NbP500 as electrolyte.

theoretic open circuit potential. It is interesting to notice that the OCV was very stable at all the three measuring temperatures over the measuring time of about 10 h. Further efforts are ongoing to improve the electrolyte and to optimize the electrodes and cell hardware in order to achieve improved fuel cell performance.

4. Conclusions

Niobium phosphates were synthesized from niobium oxide and phosphoric acid. The existence of proton-containing groups in the phosphates was verified and the groups were found to be preserved after heat treatment at temperatures above 500 °C and contribute to the proton conductivity, which was found to be of the 10^{-2} S cm^{-1} level at 250 °C under a dry atmosphere. Higher conductivities were achieved by introduction of water vapour to the atmosphere and reached 5.8×10^{-2} S cm^{-1} under pure water vapour at the same temperature. The prepared conductors showed good stability during a test of up to 50 h under both dry and slightly humidified atmospheres. EMF measurements confirmed the protonic nature of the ionic conductivity and a stable OCV of 1.045 V was obtained. Thus niobium phosphate shows potential as an electrolyte material for intermediate temperature fuel cell applications.

Acknowledgements

Funding of this work is acknowledged from the Danish National Research Foundation (the PROCON Center), the Danish Council for Strategic Research (MEDLYS), the National Natural Science Foundation of China (21011130027, International (Regional) Cooperation and Exchange program) and the National Basic Research Program of China (973 Program, 2012CB932800).

Notes and references

1 S. M. Haile, D. A. Boysen, C. R. I. Chisholm and R. B. Merle, *Nature*, 2001, **410**, 910–913.
2 D. A. Boysen, S. M. Haile, H. J. Liu and R. A. Secco, *Chem. Mater.*, 2003, **15**, 727–736.
3 D. A. Boysen, T. Uda, C. R. I. Chisholm and S. M. Haile, *Science*, 2004, **303**, 68–70.
4 P. Heo, K. Ito, A. Tomita and T. Hibino, *Angew. Chem., Int. Ed.*, 2008, **47**, 7841–7844.
5 X. Chen, X. Li, S. Jiang, C. Xia and U. Stimming, *Electrochim. Acta*, 2006, **51**, 6542–6547.
6 K. Suzuki and S. Hayashi, *Phys. Rev. B: Condens. Matter*, 2006, 73.
7 S. M. Haile, C. R. I. Chisholm, K. Sasaki, D. A. Boysen and T. Uda, *Faraday Discuss.*, 2007, **134**, 17–39.
8 B. C. H. Steele and A. Heinzel, *Nature*, 2001, **414**, 345–352.
9 K. D. Kreuer, *Chem. Mater.*, 1996, **8**, 610–641.
10 P. Heo, N. Kajiyama, K. Kobayashi, M. Nagao, M. Sano and T. Hibino, *Electrochem. Solid-State Lett.*, 2008, **11**, B91–B95.
11 M. Nagao, T. Kamiya, P. Heo, A. Tomita, T. Hibino and M. Sano, *J. Electrochem. Soc.*, 2006, **153**, A1604–A1609.
12 Y. C. Jin, Y. B. Shen and T. Hibino, *J. Mater. Chem.*, 2010, **20**, 6214–6217.
13 Y. B. Shen, M. Nishida, W. Kanematsu and T. Hibino, *J. Mater. Chem.*, 2011, **21**, 663–670.
14 O. Paschos, J. Kunze, U. Stimming and F. Maglia, *J. Phys.: Condens. Matter*, 2011, **23**, 234110.
15 I. Nowak and M. Ziolek, *Chem. Rev.*, 1999, **99**, 3603–3624.
16 M. Ziolek, *Catal. Today*, 2003, **78**, 47–64.
17 K. Tanabe, *Catal. Today*, 1990, **8**, 1–11.
18 Z. Chen, T. Iizuka and K. Tanabe, *Chem. Lett.*, 1984, 1085–1088.
19 K. Tanabe and S. Okazaki, *Appl. Catal., A*, 1995, **133**, 191–218.
20 T. Iizuka, K. Ogasawara and K. Tanabe, *Bull. Chem. Soc. Jpn.*, 1983, **56**, 2927–2931.
21 J. C. G. Da Silva, S. Folgueras-Dominguez and A. C. B. Dos Santos, *J. Mater. Sci. Lett.*, 1999, **18**, 197–200.
22 T. Armaroli, G. Busca, C. Carlini, M. Giuttari, A. M. R. Galletti and G. Sbrana, *J. Mol. Catal. A: Chem.*, 2000, **151**, 233–243.
23 A. Florentino, P. Cartraud, P. Magnoux and M. Guisnet, *Appl. Catal., A*, 1992, **89**, 143–153.
24 J. F. Zhu and Y. N. Huang, *Inorg. Chem.*, 2009, **48**, 10186–10192.
25 S. Okazaki, M. Kurimata, T. Iizuka and K. Tanabe, *Bull. Chem. Soc. Jpn.*, 1987, **60**, 37–41.
26 T. Kushimoto, Y. Ozawa, A. Baba and H. Matsuda, *Catal. Today*, 1993, **16**, 571–578.
27 M. Cantero, L. M. Real, S. Bruque, M. M. Lara and J. R. R. Barrado, *Solid State Ionics*, 1992, **51**, 273–279.
28 Z. Chai, D. Dong, C. Wang, H. Zhang, P. A. Webley, D. Zhao and H. Wang, *J. Membr. Sci.*, 2010, **356**, 147–153.
29 S. W. Tao, *Solid State Ionics*, 2009, **180**, 148–153.
30 A. Tomita, N. Kajiyama, T. Kamiya, M. Nagao and T. Hibino, *J. Electrochem. Soc.*, 2007, **154**, B1265–B1269.
31 A. Chahine, M. Et-tabirou and J. L. Pascal, *Mater. Lett.*, 2004, **58**, 2776–2780.
32 S. H. Im, Y. H. Na, N. J. Kim, D. H. Kim, C. W. Hwang and B. K. Ryu, *Thin Solid Films*, 2010, **518**, E46–E49.
33 X. X. Xu, S. W. Tao, P. Wormald and J. T. S. Irvine, *J. Mater. Chem.*, 2010, **20**, 7827–7833.
34 X. Sun, S. Wang, Z. Wang, X. Ye, T. Wen and F. Huang, *Solid State Ionics*, 2008, **179**, 1138–1141.
35 X. Wu, A. Verma and K. Scott, *Fuel Cells*, 2008, **8**, 453–458.

